HHS Public Access

Author manuscript

Mucosal Immunol. Author manuscript; available in PMC 2013 November 20.

Published in final edited form as:

Mucosal Immunol. 2013 January ; 6(1): 69–82. doi:10.1038/mi.2012.49.

IL-22 from conventional NK cells is epithelial regenerative and inflammation protective during influenza infection

Pawan Kumar, PhD[1], **Monica S Thakar, MD**[1,2], **Wenjun Ouyang, PhD**[3], and **Subramaniam Malarkannan, PhD**[1,4,5,¥]

[1]Laboratory of Molecular Immunology and Immunotherapy, Blood Research Institute, 8727 Watertown Plank Road, Milwaukee, WI 53226

[2]Department of Pediatrics, Medical College of Wisconsin, Milwaukee, WI 53226

[3]Genentech Inc, South San Francisco, CA 94080, USA

[4]Department of Medicine, Medical College of Wisconsin, Milwaukee, WI 53226

[5]Department of Microbiology and Molecular Genetics, Medical College of Wisconsin, Milwaukee, WI 53226

Abstract

Influenza infection primarily targets the upper respiratory system, leading to a severe destruction of the epithelial cell layer. The role of immune cells in the regeneration of tracheal and bronchial epithelial cells is not well defined. Here, we investigated the production of pro-constructive cytokine, Interleukin-22 (IL-22), in the bronchoalveolar lavage (BAL), trachea, lung tissue, and spleen during influenza infection. We found that conventional NK cells ($NCR1^{+}NK1.1^{+}CD127^{-}ROR\gamma t^{-}$) were the predominant IL-22-producers in the BAL, trachea and lung tissues. Tracheal epithelial cells constitutively expressed high levels of IL-22R and underwent active proliferation in response to IL-22 in the wild type (WT) mice. Infection of *IL-22*$^{-/-}$ mice with influenza virus resulted in a severe impairment in the regeneration of tracheal epithelial cells. In addition, *IL-22*$^{-/-}$ mice continued to lose body weight even after 10 days post infection (DPI 10) without any recovery. Tracheal epithelial cell proliferation was significantly reduced in *IL-22*$^{-/-}$ mice during influenza infection. Adoptive transfer of IL-22 sufficient but not IL-22 deficient NK cells into *IL-22*$^{-/-}$ mice restored the tracheal/bronchial epithelial cell regeneration and conferred protection against inflammation. Our findings strongly suggest that conventional NK cells have evolved to both kill virus-infected cells and also to provide vital cytokines for tissue regeneration.

¥To whom correspondence should be addressed (Subra.malar@bcw.edu).

Authors Contributions:

PK performed all the experiments. WO provided critical reagents. PK, MT and SM designed the experiments, analyzed data and wrote the manuscript.

Conflict of interest: The authors claim no financial conflict of interest.

INTRODUCTION

NK cells play a crucial role through cytotoxicity and by producing inflammatory cytokines during influenza infection[1, 2]. However, their unique abilities in promoting tracheal and bronchial epithelial cell regeneration in the lung are not fully understood. Infection with influenza virus causes a high degree of morbidity and mortality[3]. Influenza infection leads to necrotizing bronchiolitis, diffuse alveolar damage, alveolar hemorrhage, and airway obliteration by severe epithelial cell destruction in human lung[4]. In particular, by primarily targeting human tracheal and apical bronchial epithelial cells[5], influenza virus severely damages these epithelial layers in the lungs of mouse[6] and human[4]. More importantly, destruction of epithelia by influenza virus and a lack of repair of this monolayer greatly augment susceptibility to secondary bacterial infections such as *Streptococcus pneumoniae*, leading to increased morbidity and mortality[7]. Thus, determining the factors involved in epithelial cell regeneration is of high clinical significance. Epithelial cells express multiple cytokine receptors such as Interleukin-1 receptor (IL-1R)[8], IL-2R[9], IL-4R[10], IL-6R[11], IL-9R[12], IL-11R[13, 14], IL-13R[15], CD120[8], and IL-22R[16]. Among these, IL-22R and its ligand, IL-22, have been shown to play a central role in the maintenance and homeostasis of gut epithelial cells[17]. Irrespective of these findings, their role in the regeneration of tracheal and bronchial epithelial cells has not been defined. Moreover, the ability of 'conventional' NK cell-derived IL-22 in epithelial cell regeneration during influenza infection has not been explored.

Various T cell subsets[18], lymphoid tissue-inducer (LTi)[19] cells, $\gamma\delta TCR^+$ T cells[20] and a subset of 'NK-like' cells[21–24] produce IL-22. The ability of conventional NK cells to produce IL-22 is contested. Both NK-like cells and 'conventional' NK cells constitutively express NCR1, also known as Nkp46, but differ in their ability to express NK1.1, CD127, and transcription factor RORγt. Conventional NK cells express abundant NK1.1 and do not express CD127 or RORγt. However, the gut-resident $CD3^-NCR1^+$ NK-like cells are negative for NK1.1 and constitutively produce IL-22[21]. These NK-like cells express IL-7 receptor α-chain, CD127, and their development strictly depends on IL-7, but not on IL-15[25]. Furthermore, unlike conventional NK cells, NK-like cells express and depend on RORγt for their development[19, 24]. In addition, the NK-like cells are $NKG2D^+$, $NKG2A^+$, c-Kit^+, $CD11b^-$, $Ly49^{Low}$, $CD122^{Low}$ and $CD69^+$ (reviewed in[26]).

In the present study, using mouse-adopted human influenza virus A/PR8/34 (PR8, H1N1), we found that conventional NK cells are fully capable of producing IL-22 in the lungs. More importantly, the conventional NK cells ($CD3^-NCR1^+NK1.1^+CD127^-ROR\gamma t^-$) are the predominant IL-22-producing cell type in the lungs of the infected mice and play a crucial role in the regeneration of tracheal and bronchial epithelial cells. In contrast to the gut, lung tissue contained negligible numbers of IL-22-producing 'NK-like' ($CD3^-NCR1^+NK1.1^-CD127^+ROR\gamma t^+$) cells. We found that influenza infection led to severe destruction of tracheal epithelial cells on DPI 4. The tracheal epithelial cells fully regenerated by DPI 15, which was dependent on the production of IL-22 from conventional NK cells. We further show that mice lacking IL-22 display a severe impairment in their ability to regenerate tracheal and bronchial epithelial cells during influenza infection. Adoptive transfer of lung-derived IL-22 sufficient but not IL-22 deficient NK cells into

IL-22$^{-/-}$ mice restored the regeneration of tracheal and bronchial epithelial cells. IL-22 sufficient but not IL-22 deficient NK cells also significantly reduced the inflammation in the lung, caused by influenza infection. Further, we found an IL-22-independent effect of donor NK cells in preventing severe weight loss during infection. These findings demonstrate for the first time that conventional NK cell-derived pro-constructive cytokine IL-22 plays a crucial role in the regeneration of epithelial cell layers during influenza infections.

RESULTS

Influenza virus infection causes significant destruction of tracheal epithelial cells

The upper respiratory tract, particularly the tracheal epithelial cells, is susceptible to influenza virus infection[6, 27]. To determine the severity of the epithelial cell destruction *in vivo*, WT mice were infected intranasally with PR8 virus at a sub-lethal dose of 5000 PFU[28]. This dose was selected since it led to significant levels of tracheal epithelial cell damage with minimal mortality in the WT mice. Although there was significant weight loss in these mice, most of them fully regained their normal body weight by DPI 15. Since the epithelial cells in the trachea are the primary targets of the PR8 virus, we first assessed the degree of tracheal epithelial cell damage during influenza infections. Towards this, we stained tracheal sections from the infected mice with E-Cadherin, which is preferentially expressed by epithelial cells, and Annexin-V to visualize the level of cell death. Tracheal sections from DPI 0 (Figure 1A) contained a continuous monolayer of columnar epithelial cells and an intact basement membrane above the cartilaginous structure. Influenza infection, however, led to the destruction of the tracheal epithelial cell barrier on DPI 4 and this resulted in the disorganization of the epithelia. This layer was strongly positive for Annexin-V on DPI 4, indicating that the infected epithelial cells were undergoing cell death, and the lumen side of the trachea lost its columnar structure (Figure 1A). However, the epithelial cell layer started to recover and fewer Annexin-V-positive cells were seen on DPI 7 and DPI 10 (Figure 1A). Similarly, E-Cadherin positive alveolar epithelial cells also underwent cell death in the apical lobe of the infected lungs (Supplementary Figure 1).

Using an infra red (IR) dye detection method developed in our laboratory[29], we also quantified the PR8 viral titers in the bronchoalveolar lavage (BAL) fluids of virus-infected mice using anti-nucleoprotein (NP) antibody (Figure 1B,C). MDCK cells were incubated with the BAL fluid or PR8 with known concentrations. The levels of virus-derived NP protein were quantified using infrared dye-conjugated antibody as a measure of viral titers (Figure 1B)[29]. Our results show that the PR8 titer peaked on DPI 4, concurrent with the highest level of tracheal epithelial cell damage observed (Figure 1C). Based on these results, we conclude that in the early phase of infection, PR8 virus causes severe damage to the tracheal epithelium.

NCR1$^+$ cells are the predominant producers of IL-22 in the BAL, lung, and spleen

IL-22 induces epithelial cell proliferation and innate defense mechanisms including the production of anti-bacterial peptides from epithelial cells[17, 30]. Earlier studies have shown that NK-like[22, 24, 31], $\alpha\beta$TCR$^+$ T[32] or $\gamma\delta$TCR$^+$ T[20, 33–35] cells can generate IL-22. Therefore, to determine the independent contributions of these cell types, we next investigated the

absolute numbers and the percentages of IL-22-producing $CD3^+$T, $CD3^+CD4^+$ T, $CD3^+CD8^+$ T, $CD3^+\gamma\delta TCR^+$ T, $CD3^-CD4^+$ LTi-like and $NCR1^+$ cells in BAL, lung tissue, and spleen of influenza-infected mice on DPI 7 (Figure 2A,B). Our data indicate that both $NCR1^+$ and $CD3^+$T cells generate IL-22 in BAL and lung tissue. However, the absolute numbers and the percentages of $IL\text{-}22^+$ $NCR1^+$ cells were significantly higher compared to that of $CD4^+$ or $CD8^+$ T cells in these tissues (Figure 2B). Indeed our data indicates these $NCR1^+$ cells can traffic into the trachea (Supplementary Figure 2A). Irrespective of the higher absolute numbers of $CD4^+$ or $CD8^+$ T compared to $NCR1^+$ cells, the absolute number of IL-22-producing $NCR1^+$ cells was significantly higher in both BAL and lung tissue (Figure 2B). Since recent studies have shown that the $\gamma\delta TCR^+$ T cells also produce IL-22 under pathological conditions[20], we compared these cells with $NCR1^+$ cells. Although we could detect considerable numbers of $\gamma\delta TCR^+$ T cells in the BAL, lung tissue, and spleen, their absolute numbers and ability in terms of IL-22 production remained significantly lower compared to $NCR1^+$ cells (Figure 2A,B).

We also tested the presence of $CD3^-CD4^+$ LTi-like cells in the BAL, lung tissue, and spleens of infected mice and found their absolute numbers are considerably negligible compared to that of $NCR1^+$ cells (Supplementary Figure 2B). Based on these findings, we conclude that a population of $NCR1^+$ cells plays a central role in the production of IL-22 during influenza infection. Analyses of $NCR1^+$ cells in different organs of non-challenged WT mice indicate the existence of considerable numbers of $NCR1^+$ cells in all the organs tested (Supplementary Figure 3A), where the lung tissue contained the maximal percentage of these cells (~5–10%). After PR8 infection, the absolute numbers of overall cell, lymphocyte, and $NCR1^+$ cell numbers were significantly increased in the lung tissues (Supplementary Figure 3B). In contrast, a continuous and significant decrease in the total lymphocytes and $NCR1^+$ NK cell numbers was observed in the spleen with progression of the disease (Supplementary Figure 3B).

IL-22-producing $NCR1^+$ cells in the lungs are conventional NK cells

Since both conventional NK and NK-like cells express NCR1, we next determined the identity of the IL-22-producing cells in the lungs of influenza-infected mice. Therefore, to determine phenotypic identity of these cells, we analyzed the expression of NCR1, NK1.1, and CD127. Our data indicate that majority of $NCR1^+$ cells in the lung tissue and spleen are $NK1.1^+$ and $CD127^-$ (Supplementary Figure 3C). To determine which one of these subsets produce IL-22, single cell suspensions of lung tissue and spleen from infected WT mice were prepared on the indicated DPI and stained for CD3, NCR1, NK1.1, and CD127, along with intracellular IL-22 (Figure 3A,B). $CD3^-NCR1^+$ cells were gated and analyzed for NK1.1 and IL-22 or CD127 and IL-22 in *ex vivo* analysis. Only a negligible number of $NCR1^+$ cells from the lung tissue produced IL-22 on DPI 0 (Figure 3A). However, a significant number of $NCR1^+$ cells were constitutively positive for IL-22 in the spleen on DPI 0. The majority of the IL-22-generating $NCR1^+$ subset in lung tissue were $NK1.1^+$ and, more importantly, they were negative for CD127 (Figure 3A,C). Similar to lung, IL-22-producing $NCR1^+$ cells in the spleen were positive for NK1.1 and negative for CD127 (Figure 3B,D). In line with these results, the $IL\text{-}22^+$ $NCR1^+$ cells present in the trachea were $NK1.1^+$ and their number peaked on DPI 4 and DPI 7 (Figure 3E,F). The specificity of

IL-22 staining was confirmed using an isotype control antibody that did not result in any detectable positive cells in the same experiment (Figure 3A,B, **Bottom panels).** During influenza infection, although no differences in the percentages of IL-22-producing cells were detected (except on DPI 10), the absolute numbers of total lymphocytes, $NCR1^+$ cells, and other subsets were significantly reduced in the spleen (Figure 3B,D).

We next investigated the expression of RORγt (anti-RORγt mAb, clone AFKJS-9) in $CD3^-NCR1^+$ cells in the lung and spleen of infected mice. $CD3^-NCR1^+$ were gated and analyzed for the expression of NK1.1 and intracellular RORγt. Interestingly, no significant RORγt positivity could be seen in the lung tissue of these mice; however, a small percentage of (3–4%) of $CD3^-NCR1^+$ become RORγt positive in the spleen of infected mice (Supplementary Figure 4A). We also did observe an increase in the $ROR\gamma t^+$ cells that were prominently $NCR1^-$ in the spleen and to a lesser extent in the lung tissue (Supplementary Figure 4B). This demonstrates that the assay conditions were optimal and that the $NCR1^+NK1.1^+$ cells are not RORγt positive in the infected lungs. To further validate our findings, we used a second RORγt-specific mAb that is derived from hybridoma clone B2D in these assays. Results using B2D confirmed that the majority of the $NCR1^+NK1.1^+$ cells in the infected lungs were RORγt negative (Supplementary Figure 4C,D). As described by earlier studies[19, 21], we have found that LPL-derived cells contain significant numbers of $ROR\gamma t^+$ cells (**data not shown**). Therefore, our results indicate that the IL-22 producing, lung-derived $NCR1^+$ cells are distinct from that of the gut in NK1.1, CD127, and RORγt expressions. Based on these studies, we conclude that the majority of the IL-22-producing $NCR1^+$ cells in the lung during influenza infection are conventional NK cells.

To further define the developmental requirement of $NCR1^+$ cells in the lungs of the influenza-infected mice, we examined their absolute numbers in *IL-15Rα*$^{-/-}$ mice. IL-15 and IL-7 are two crucial cytokines that play an important role in the development of different NK subsets[25, 36]. Lack of IL-15 severely reduces the number of conventional NK cells[25]. However, its absence did not affect the development of the gut-resident NK-like ($NCR1^+NK1.1^-CD127^+ROR\gamma t^+$) subset[25]. To investigate the cytokine requirements of the lung-derived conventional NK cells ($NCR1^+NK1.1^+ROR\gamma t^-$), we used *IL-15Rα*$^{-/-}$ mice. As described earlier[37], lack of IL-15Rα did not affect the total cell counts or absolute lymphocyte numbers in the lung or spleen (Supplementary Figure 5A). However, the absolute numbers and percentages of $CD3^-NCR1^+$ cells were significantly reduced in the lung, MLN, and spleen, but not in the LPL (Supplementary Figure 5A,B). In addition, the absolute numbers of conventional NK cells ($NCR1^+NK1.1^+CD127^-$) in the lung and spleen of *IL-15Rα*$^{-/-}$ mice were significantly reduced as compared to those of WT littermates (Supplementary Figure 5C). Based on these results, we conclude that the IL-22 producing, $NCR1^+$ conventional NK cells in the lung depend on IL-15 for their development. Also, we found induction of abundant expression of IL-23R in these lung-derived conventional NK cells, which provides a possible mechanism by which IL-22 production is induced in these cells (Supplementary Figure 5D).

Lack of IL-22 results in persistent tracheal damage and reduced epithelial cell proliferation

To further validate the role of IL-22 in tracheal epithelial cell regeneration, we infected the WT and *IL-22*$^{-/-}$ mice with PR8. NK cells develop normally in *IL-22*$^{-/-}$ mice and their absolute numbers were comparable to that of WT (**data not shown**). Lungs, along with trachea, from the infected mice were removed on different DPI, mounted, stained with Hematoxylin and Eosin, and analyzed for the extent of epithelial cell damage. To statistically evaluate the loss of epithelial cell layers, we used a single cartilage length as one unit (100%) and calculated the percent epithelial layer loss on different DPI (Supplementary Figure 6). Using this method, tracheal epithelial cell loss was measured in WT and *IL-22*$^{-/-}$ mice for each DPI. Data presented in Supplementary Figure 7 (Top panels) demonstrates that significant loss of epithelial layer occurred on DPI 4 in the WT mice. In these infected mice, the epithelial layer started to recover on DPI 7 and the damage was progressively reduced (Supplementary Figure 7A,B). Tracheal sections from DPI 7 and DPI 10 show substantial regrowth and recovery of the epithelial cell layer. However, in contrast to WT mice, *IL-22*$^{-/-}$ mice failed to regenerate their epithelial layers by DPI 15 (Supplementary Figure 7A,B). Moreover, the damaged mature epithelial cells were largely replaced by a single stratified layer of atypical cells (flat epithelial atypia) at later DPI (Supplementary Figure 7A, middle panels). Statistical analyses of tracheal damage per cartilage length revealed that the lack of IL-22 significantly reduced the regenerative potentials of epithelial cells in the *IL-22*$^{-/-}$ mice compared to that of WT (Supplementary Figure 7B). In addition to the tracheal epithelial cells, the PR8 infection led to significant alterations in the lung tissue. Histopathological analyses of lung tissues from the infected WT and *IL-22*$^{-/-}$ mice showed severe bronchiolitis with perivasculitis, alveolitis, and increased leukocyte infiltrations (**Arrowheads**, Supplementary Figure 8).

Our study shows that influenza infections result in extensive epithelial cell damage. In turn, remaining uninfected epithelial cells proliferate to repair damage. Therefore, we next analyzed the expression of IL-22R and the rate of proliferation in *IL-22*$^{-/-}$ mice at different DPI. Towards this, tracheal sections were analyzed for the expression of IL-22R and the proliferation marker Ki-67. IL-22R is equally expressed on tracheal epithelial cells on both apical and basal sides in WT and *IL-22*$^{-/-}$ mice (Figure 4A–C). The epithelial cell layer became disorganized and damaged with continued viral infection on DPI 4, in both WT and *IL-22*$^{-/-}$ mice. Interestingly, in the trachea of WT mice, a considerable number of epithelial cells became positive for Ki-67 on DPI 4, indicating the start of cell division in the epithelial layer. However, only a minimal number of Ki-67 cells could be detected in the *IL-22*$^{-/-}$ mice (Figure 4A–C). Flow cytometry analyses of IL-22R expression in the E-Cadherin^{+} tracheal epithelial cells did not reveal any significant differences between the WT and *IL-22*$^{-/-}$ mice (Figure 4B). However, compared to WT, the trachea of *IL-22*$^{-/-}$ mice contained significantly reduced percentages of Ki-67^{+} epithelial cells on DPI 7 (Figure 4C). Based on our observations, we conclude that IL-22 indeed plays a critical role in the regeneration of tracheal epithelial cells.

Adoptive transfer of IL-22 sufficient NK cells is epithelial regenerative and inflammation protective

To determine the exclusive role of conventional NK cells in the regeneration of tracheal epithelial cells, we sorted $CD3^-$ $NK1.1^+NCR1^+$ NK cells from the lung of B6.SJL ($CD45.1^+$) mice and adoptively transferred (1×10^6/mice) into influenza-infected *IL-22*$^{-/-}$ mice ($CD45.2^+$) on DPI 4 (Figure 5A). One day after the adoptive transfer, $CD45.1^+$ donor NK cells could be detected in the PR8- infected host BAL fluid and spleen (Figure 5B). Most importantly, a subset of the $CD45.1^+$ donor NK cells in the host BAL fluid and spleen were IL-22 positive (Figure 5B,C). Confocal microscopic analyses of infected host lung sections revealed the presence of IL-22-producing $CD45.1^+NCR1^+$ donor cells (Figure 5D, E). Additionally, evaluations in multiple confocal microscopic fields further confirmed that only the donor ($CD45.1^+$) but not the recipient ($CD45.2^+$) NK cells produced IL-22 one day (Figure 5F) or three days (Figure 5G) after adoptive transfer.

Next, we investigated whether adoptive transfer of donor NK cells can rescue the *IL-22*$^{-/-}$ mice from severe weight loss and epithelial cell damage. PR8 infection led to severe loss of body weight in both WT and *IL-22*$^{-/-}$ mice (Figure 6A). On DPI 4, these mice lost more than 10% of their total body weight. By DPI 10, WT mice started to recover, while the *IL-22*$^{-/-}$ mice failed to display any improvement and continued to lose body weight (Figure 6A). Transfer of IL-22 sufficient NK cells into *IL-22*$^{-/-}$ mice prevented severe weight loss (Figure 6B). Most of these mice displayed only minimal weight loss and fully recovered their weight after adoptive transfer. However, this recovery can also be attributed to increased levels of effector functions such as cytotoxicity and anti-viral cytokine production by the donor NK cells. Therefore, to determine the precise role of IL-22 in the recovery of the infected mice, we adoptively transferred IL-22 deficient NK cells into *IL-22*$^{-/-}$ mice. It is important to note that the IL-22 deficient NK cells developed and matured normally (data not shown). Moreover, they displayed comparable levels of cytotoxicity against $H60^+$ target cells and production of IFN-γ, GM-CSF, TNF-α, MIP-1α, MIP-1β and RANTES to their WT counter parts (Kumar and Malarkannan, unpublished). Transfer of these IL-22 deficient NK cells into *IL-22*$^{-/-}$ mice following influenza infection resulted in only moderate weight loss compared to that of *IL-22*$^{-/-}$ mice receiving IL-22 sufficient NK cells (Figure 6B). This implies that an IL-22-independent effect of donor NK cells control the severity of the weight loss during infection. Microscopic analyses of tracheal sections on DPI 7 and DPI 15 revealed that the adoptive transfer of one million IL-22 sufficient lung-derived NK cells significantly reduced the epithelial layer damage (Figure 6C,D). Transfer of IL-22 sufficient NK cells fully restored the regenerative abilities of the epithelial monolayer. By DPI 15, the epithelial layers were fully restored with only a minimal residual damage (Figure 6D). In contrast, *IL-22*$^{-/-}$ mice that were infused with IL-22 deficient NK cells failed to regenerate their tracheal epithelial cell layers. Tracheal sections derived from both DPI 7 and DPI 15 displayed persistent epithelial damage (~30%) as seen in the *IL-22*$^{-/-}$ mice (Figure 6D).

Using confocal microscopy, we analyzed tracheal epithelial cell proliferation by staining for Ki-67 (red) along with IL-22R (green) (Figure 7A). Infusion of IL-22 sufficient NK cells into the infected *IL-22*$^{-/-}$ mice resulted in an increase in the Ki-67 positive epithelial cells. However, trachea from *IL-22*$^{-/-}$ mice that were infused or not with IL-22 deficient NK cells

showed a considerable decrease in Ki-67 positivity (Figure 7A). We also analyzed the status of bronchial epithelial cells in these mice. Hematoxylin and Eosin staining of the lung tissue revealed that the adoptive transfer of IL-22 sufficient NK cells improved the regeneration of the bronchial epithelial cell layer in *IL-22*$^{-/-}$ mice as evidenced from DPI 7 and DPI 15 tissue sections (Figure 7B). Conversely, both *IL-22*$^{-/-}$ mice and IL-22 deficient NK cell-infused *IL-22*$^{-/-}$ mice failed to regenerate their epithelial layer (Figure 7B, **exploded views**). To further determine the degree of pathology in the lungs, we quantified the levels of collagen fiber deposition as a measure of inflammation. Masson's trichrome staining showed a considerable increase in collagen deposition in the lung tissues of *IL-22*$^{-/-}$ mice compared to that of WT (Figure 8A). Infusion of IL-22 sufficient NK cells significantly reduced the levels of collagen deposition and the associated pathology score (Figure 8B). However, infusion of IL-22 deficient NK cells did not reduce the severity of inflammation in the lung tissue and was similar to that of *IL-22*$^{-/-}$ mice (Figure 8A,B). Based on this data, we conclude that conventional NK cells in the lung play both a protective and a pro-regenerative role.

DISCUSSION

Tracheal epithelial cells are the major targets of many respiratory viruses[6, 38]. A successful entry of these viruses into the epithelial cells leads to viral multiplication and eventual destruction of this layer[39]. Therefore, a rapid regeneration of this protective barrier is extremely critical to prevent secondary opportunistic bacterial infections[7]. Indeed, loss of ciliary activity and destruction of the epithelial cell layer leads to increased risk of bacterial infections that cause severe pneumonia, which could be fatal[7]. In this context, the role of IL-22 in tracheal epithelial cell homeostasis during viral infection has not been investigated. Here, we demonstrate that tracheal epithelial cells constitutively express abundant levels of IL-22R. PR8-mediated infection extensively damages the epithelial monolayer. More importantly, our findings are first to demonstrate that IL-22-derived from conventional NK cells-derived is crucial for the regeneration of tracheal and bronchial epithelial cells.

In this study, we establish that the IL-22-producing, NCR1^{+} cells in the trachea and lungs of the infected mice possess a conventional NK cell phenotype and differ from the LTi-like or NK-like subset defined in the gut. Existing paradigms define IL-22-generating NCR1^{+} cells as a novel LTi-like subset that exhibit NCR1^{+}NK1.1^{-} CD127^{+}RORγt^{+} phenotype[19, 21, 23, 26]. These gut resident cells are characterized by three essential features. First, the NK-like cells predominantly found in the intestinal lamina propria depend on IL-7 for their development but not IL-15[25]. Unique expression of IL-7 receptor chain α (CD127) in these cells helps to identify them among other innate cells[25]. In contrast to this, our study shows that the IL-22-producing cells in the influenza-infected lungs lacked CD127 expression. The expression of pan NK cell marker NK1.1 (CD161)[40] was reported to be notably low or negative in a significant proportion of IL-22^{+} NK-like subset in the gut[21, 23]. However, in our study, we did not find a similar phenotypic population in the lungs of influenza-infected mice. In contrast to the observations made in the gut, the lung-derived IL-22^{+} cells were predominantly positive for NK1.1. Similar to LTi cells, expression of transcription factor RORγt is obligatory for the development and functions of NK-like cells in the gut[24, 41]. However, we failed to detect any expression of RORγt in the lung-derived,

IL-22-producing, NCR1^{+}NK1.1^{+} cells; thereby, indicating their dependence on a developmental pathway similar to that of conventional NK cells. Based on these observations, we conclude that the lung-derived IL-22-generating cells are NK1.1^{+} and RORγt^{-} and, therefore, are conventional NK cells.

Earlier studies have shown that the development and functions of conventional NK cells depend on IL-15 and both *IL-15*$^{-/-}$ and the *IL-15R*$\alpha^{-/-}$ mice lack these cells[42]. Unlike conventional NK cells, the development of gut-derived NK-like cells do not depend on IL-15 as evidenced by their normal numbers in *IL-15*$^{-/-}$ mice[25]. Conversely, our studies using *IL-15R*$\alpha^{-/-}$ mice found that IL-22-producing, NCR1^{+} lung cells were absent in these mice, further confirming that these cells are conventional NK cells. On the contrary, a recent study described reduced mortality in *IL-15*$^{-/-}$ mice after challenge with A/FM/1/47 (H1N1) virus that was attributed to a significant reduction in the antigen-specific CD8^{+} T cells with no alterations in viral titers or inflammatory cytokines (TNF-α and IL-6)[43]. However, this study did not investigate the status of epithelial cell damage, subsequent regeneration, and the role of IL-22. It is also important to note that the lack of IL-15Rα has been implicated in enhanced production of IL-10[44]. Thus, an overall reduction in the mortality could be attributed to a reduced recruitment of T cells that results in significantly less inflammation and pathogenesis. This is further confirmed by the fact that the over-expression of IL-15 is associated with autoimmune intestinal damage and celiac disease[45]. Earlier studies have also shown that the gut-derived NK-like cells are NKG2D^{+}, NKG2A^{+}, c-Kit^{+} and CD69^{+} [26]. Most importantly, unlike conventional NK cells, these NK-like cells were CD11b^{-}, Ly49^{Low}, CD122^{Low} [26]. While we found that the lung-derived IL-22-producing, conventional NK cells expressed comparable levels of NKG2D, NKG2A, and CD69, there was a significant increase in the expression of c-Kit. The expression of CD11b, CD122 and various Ly49 receptors were largely unaltered (**data not shown**).

Regeneration of epithelial cells is crucial to maintain lung homeostasis. In adult human trachea, cell turnover is considerably low[46]. However, epithelial injury initiates rapid proliferation of surviving cells[47]. Infection of C57BL/6 mice with influenza resulted in epithelial cell damage and eventual regeneration through vigorous proliferation starting from DPI 7, as indicated by their expression of proliferating cell nuclear antigen (PCNA)[39]. However, factors that induce the proliferation of lung epithelial cells were not defined. Although earlier studies described the possible production of IL-22 from NK cells, they did not correlate the IL-22 function to epithelial cell regeneration[30, 48, 49]. Our results show that the lack of IL-22 significantly impaired the regenerative potentials of tracheal epithelial cells as indicated by Ki-67 staining. This nuclear protein is a cell proliferation marker that can be exclusively detected inside the nucleus during interphase. Ki-67 is present during G_1, S, G_2, and mitotic phases, but is absent from resting cells (G_0)[50]. Thus, IL-22 is critical for the regeneration of epithelial cells after injury caused by viral infections and corroborate with earlier studies, where activation via IL-22R results in epithelial cell survival, proliferation and IL-10 release[51]. Additionally, epithelial cells also produce anti-microbial proteins such as β-defensins and S100As in response to IL-22[23]. Expression of IL-22R was not altered in the *IL-22*$^{-/-}$ mice, excluding a potential auto-regulatory role for IL-22 in its receptor expression. We found additional cells that were positive for IL-22R in the infected mice

between the basement membrane and the cartilaginous structures; however, their identities are currently not known. These cells could possibly be basal stem cells that are differentiating, which would eventually give rise to mature epithelial cells.

A recent study has suggested that *in vivo* neutralization of IL-22 using antibodies did not alter the pattern of body weight loss during influenza infection[52]. However, this study failed to demonstrate that the anti-IL-22 antibody treatment fully neutralized the functions of IL-22. In our study, adoptive transfer of IL-22-sufficient NK cells from the donor on DPI 4, significantly reduced the weight loss in the *IL-22*$^{-/-}$ mice. Interestingly, adoptive transfer of IL-22-deficient NK cells also conferred protection against weight loss, indicating an IL-22 independent effect of donor NK cells. Further studies are required to precisely determine the molecular basis of this protective phenomenon of NK cells. Adoptive transfer of IL-22-sufficient but not IL-22-deficient NK cells restored the regenerative potentials of epithelial cells in *IL-22*$^{-/-}$ mice. This could be due to the fact that IL-22 induces antimicrobial peptides[17, 53], which in turn helped to reduce the severity of influenza virus infections. Moreover, IL-22 can also stimulate the production of anti-inflammatory IL-10 from epithelial cells[51]. In turn, IL-10 can reduce the entry of inflammatory lymphocytes into the lung through a negative feedback. Our present study sets the stage for clinical immunotherapies, such as administration of IL-22 or IL-22-producing NK cells for patients requiring rapid regeneration of epithelial cell layers. This includes pulmonary complications, burn victims, or patients who develop severe graft-versus-host disease after donor-derived bone marrow transplantations. In these patients, a local or a systemic administration of IL-22 may accelerate epithelial cell regeneration and the production of antimicrobial peptides to efficiently prevent secondary opportunistic infections.

METHODS

Mice, virus and cell-lines

The C57BL/6 (WT), *IL-15Rα*$^{-/-}$ and B6.SJL (CD45.1) mice were obtained from The Jackson Laboratory (Bar Harbor, ME). Generation of *IL-22* gene knockout mice has been described earlier[17]. All mice were maintained in pathogen-free conditions at the Biological Resource Center (BRC) of the Medical College of Wisconsin (MCW), Milwaukee, WI. All animal protocols used were approved by the MCW IACUC. Madin-Darby Canine Kidney (MDCK) cells were purchased from ATCC (Rockville, MD) and cultured in RPMI 1640 medium with 10% FBS. Mouse adapted human influenza virus A/PR/8/34 (PR8) was (a kind gift from Dr Thomas M Moran, Mount Sinai School of Medicine, NY) used as described[54].

In vivo infection and BAL fluid collection

WT mice 6–8 weeks of age were deeply anesthetized and were intranasally challenged with 5000 PFU of PR8 virus in sterile PBS in a total volume of 30 μl through one nostril. Mock infections were carried out using only sterile PBS without the virus. After infections, mice were euthanized and thoracic cavity was cut open and a 1 cm incision was made parallel to the trachea through the fur of the mouse to expose it. A midline incision was made on the ventral aspect of the trachea slightly above the thoracic inlet. 0.3 ml of PBS-1% BSA was

infused into lung through the thoracic inlet using a sterile 1 ml syringe. Lavage fluid was aspirated, aliquoted and frozen until use.

Lung pathology

To determine the levels of epithelial damage, cryosections from PR8-infected mice were stained with Hematoxylin and Eosin. Levels of lung pathology were determined by collagen deposition using Masson's trichrome staining. Severity of lung pathology was quantified in a double-blind method based on the intensity of staining in a scale of 1 to 10, where 10 being the highest. To statistically quantify the epithelial damage each cartilage length was taken as a single unit (100%) from which the percent damage was measured (Supplementary Figure 6). Images of trachea were obtained at 10× magnification using light microscopy, images were printed and total lengths of individual cartilages were measured and compared with lengths of respective tracheal regions where epithelial cells were missing or damaged. Percent damage was calculated as (Length of the tracheal region with epithelial damage/ Respective Individual cartilage length)× 100. Multiple individual cartilages were analyzed for each DPI. Images of lung tissues were obtained at 10× magnification using the same microscope and the pathology was evaluated.

Detection of viral nucleoprotein (NP) by LI-COR Odyssey

Infra Red (IR) dye-based methodology was standardized in our laboratory to quantify the influenza viral titers in unknown samples[29]. Briefly, MDCK cells were cultured in optical flat bottom black 384-well plates, washed twice with serum free DMEM medium containing 0.2% BSA, 100 U/ml penicillin, 100 μg/ml streptomycin, 1 mM sodium pyruvate, 5% sodium bicarbonate solution and 0.001% β-mercaptoehanol. MDCK cells were incubated with 10 μl of BAL fluid that was collected on different DPI or control PR8 virus with known PFU in 10 μl (384-well plate) medium-containing L-1-tosylamido-2-phenylethyl chloromethyl ketone (TPCK)-treated trypsin (0.2 μg/ml). Following 1 h of infection, an additional 40 μl of 10% FBS-containing medium was added to each well. After 16 h of infection, cells were washed twice for 5 min with PBS-containing 1% BSA and fixed with 1% paraformaldehyde. After blocking, infected cells were stained with anti-NP antibody (1:1000, Clone# V232208, CDC). Cells were washed and incubated for 1 h with goat anti-mouse IRDye@800 secondary antibody (1:200, LI-COR, Lincoln, NE). Plates were scanned using 780 nM for detection and 680 nM channels as reference in LI-COR Odyssey IR scanner (LI-COR, Lincoln, NE).

Lymphocyte and epithelial cell preparations

Single cell suspensions from various tissues were prepared and used for different analyses. Briefly, lungs were minced into pieces and digested with 500 μl of 10 mg/ml collagenase (C5138, 100 mg, Sigma, St Louis, MO, USA) and 50 μl of 200 IU of DNase I from bovine pancreas (D4527-20KU, Sigma, St Louis, MO, USA) in total volume of 5 ml of RPMI1640 complete medium for 1 h at 37° C. Lymphocytes from the lung were isolated by Ficoll-Hypaque density gradient. To separate lymphocytes from the gut, tissue pieces (1–1.5cm) were incubated with trypsin-EDTA to separate intra-epithelial lymphocytes (IEL)[55]. Tissue fragments were digested with 500 μl of 10 mg/ml collagenase and 50 μl of 200 IU of DNase I. LPLs were further purified using discontinuous Percoll gradient (40% and 80%; Sigma, St

Louis, MO, USA). For epithelial cell isolation, trachea was digested in dispase (5mg/ml, Stem Cell Technologies) for 15 minutes followed by 10 minutes incubation in trypsin-EDTA at 37° C.

Flow cytometry

Flow cytometry was performed as described earlier[56, 57]. Single cell preparations from spleen, trachea, lung and LPL were surface stained with CD3ε (145–2C11), NK1.1 (PK136), NCR1 (29A1.4), CD127 (A7R34), γδTCR (GL3) (eBioscience, San Diego, CA), and IL-23R (258010) and E-Cadherin (R & D System, Minneapolis, MN). For intracellular staining, single-cell suspensions from lung or BAL or spleen or trachea were first stain for surface receptor for 30 min followed by fixation (Fixation buffer, BioLegend Inc. San Diego, CA), and permeabilization (Permeabilization wash buffer, BioLegend Inc. San Diego, CA) steps for additional 20 min. Cells were stained intracellularly with PE-conjugated IL-22 (140301) (R & D System, Minneapolis, MN) or RORγt (AFKJS-9, B2D) (eBioscience, San Diego, CA) or Ki-67 (Abcam, Cambridge, MA) in permeabilization wash buffer and analyzed in LSR-II (BD Biosciences, San Jose, CA).

Confocal microscopy

Confocal microscopy was performed as described earlier[58]. To detect IL-22$^+$ donor NK cells following adoptive transfer, lung cryosections were stained with anti-mouse -CD45.1-Alexa Flour 488 (donor), -CD45.2-Pacific Blue (host), -NCR1-APC and -IL-22-PE. Respective isotype controls were used to confirm the specificity of stainings. Lung cryosections from PR8-infected mice were also stained for rabbit anti-E-Cadherin (Cell Signaling Technology, Danvers, MA) and anti-Annexin-V (BD Biosciences, San Diego, CA) or rat anti-IL-22R (R&D System, Minneapolis, MN) and rabbit anti-Ki-67 (Abcam, Cambridge, MA) overnight. After three washes cryosections were stained with respective Alexa Fluor-conjugated secondary antibody for 1 h. Images were obtained using Olympus FluoView FV1000 MPE microscope (Olympus, Center Valley, PA, USA).

Adoptive transfer

Single cell suspensions from the lungs of B6.SJL (H-2^b, CD45.1$^+$) or *IL-22*$^{-/-}$ mice were produced and the lymphocytes were isolated on a Ficoll density gradient. These lymphocyte preparations were stained with anti-CD3, anti-NCR1 and anti-NK1.1 monoclonal antibodies. CD3$^-$ NCR1$^+$NK1.1$^+$ conventional NK cells were sorted and cultured in 1000 U of IL-2 for 8–12 days. 1 × 10^6 cells were adoptively transferred into *IL-22*$^{-/-}$ (CD45.2) on DPI 4, intravenously. Donor CD45.1$^+$ NK cells were detected and the generation of IL-22 was analyzed following day 1 and day 3 post adoptive transfer by flow cytometry and confocal microscopy.

Statistics

Statistical analyses were performed using the two-tailed, unpaired, Student's t-test. *P* values that were ≤ 0.05 were considered significant.

Supplementary Material

Refer to Web version on PubMed Central for supplementary material.

Acknowledgments

We thank Drs James Di Santo and Andreas Diefenbach for expert opinions. We are indebted to Tina Heil, Kristina Schuldt and Rajasekaran Kamalakannan for the critical reading of this manuscript. We thank the members of our laboratory for critical discussions. This work is supported in part by NIH grant R01 A1064828 (to S.M.) and Hyundai Scholars Program, Rebecca Jean Slye Endowment, Clinical and Translational Science Institute and American Cancer Society Pilot Research Grant (to MST).

Reference List

1. Mandelboim O, et al. Recognition of haemagglutinins on virus-infected cells by NKp46 activates lysis by human NK cells. Nature. 2001; 409:1055–1060. [PubMed: 11234016]
2. Achdout H, et al. Enhanced recognition of human NK receptors after influenza virus infection. J Immunol. 2003; 171:915–923. [PubMed: 12847262]
3. Gill JR, et al. Pulmonary pathologic findings of fatal 2009 pandemic influenza A/H1N1 viral infections. Arch Pathol Lab Med. 2010; 134:235–243. [PubMed: 20121613]
4. Capelozzi VL, et al. Pathological and ultrastructural analysis of surgical lung biopsies in patients with swine-origin influenza type A/H1N1 and acute respiratory failure. Clinics (Sao Paulo). 2010; 65:1229–1237. [PubMed: 21340209]
5. Matrosovich MN, Matrosovich TY, Gray T, Roberts NA, Klenk HD. Human and avian influenza viruses target different cell types in cultures of human airway epithelium. Proc Natl Acad Sci U S A. 2004; 101:4620–4624. [PubMed: 15070767]
6. Pekosz A, Newby C, Bose PS, Lutz A. Sialic acid recognition is a key determinant of influenza A virus tropism in murine trachea epithelial cell cultures. Virology. 2009; 386:61–67. [PubMed: 19195676]
7. Kash JC, et al. Lethal synergism of 2009 pandemic H1N1 influenza virus and Streptococcus pneumoniae coinfection is associated with loss of murine lung repair responses. MBio. 2011; 2
8. Harder J, et al. Mucoid Pseudomonas aeruginosa, TNF-alpha, and IL-1beta, but not IL-6, induce human beta-defensin-2 in respiratory epithelia. Am J Respir Cell Mol Biol. 2000; 22:714–721. [PubMed: 10837369]
9. de Paiva CS, et al. Cleavage of functional IL-2 receptor alpha chain (CD25) from murine corneal and conjunctival epithelia by MMP-9. J Inflamm (Lond). 2009; 6:31. [PubMed: 19878594]
10. Colgan SP, et al. IL-4 directly modulates function of a model human intestinal epithelium. J Immunol. 1994; 153:2122–2129. [PubMed: 7914217]
11. Barasch J, et al. Mesenchymal to epithelial conversion in rat metanephros is induced by LIF. Cell. 1999; 99:377–386. [PubMed: 10571180]
12. Vermeer PD, Harson R, Einwalter LA, Moninger T, Zabner J. Interleukin-9 induces goblet cell hyperplasia during repair of human airway epithelia. Am J Respir Cell Mol Biol. 2003; 28:286–295. [PubMed: 12594054]
13. Deutscher N, et al. Functional expression of the interleukin-11 receptor alpha-chain in normal colonic epithelium and colon cancer. Int J Colorectal Dis. 2006; 21:573–581. [PubMed: 16292518]
14. Kiessling S, et al. Functional expression of the interleukin-11 receptor alpha-chain and evidence of antiapoptotic effects in human colonic epithelial cells. J Biol Chem. 2004; 279:10304–10315. [PubMed: 14701802]
15. Morimoto M, et al. Functional importance of regional differences in localized gene expression of receptors for IL-13 in murine gut. J Immunol. 2006; 176:491–495. [PubMed: 16365442]
16. Wolk K, Sabat R. Interleukin-22: a novel T- and NK-cell derived cytokine that regulates the biology of tissue cells. Cytokine Growth Factor Rev. 2006; 17:367–380. [PubMed: 17030002]

17. Zheng Y, et al. Interleukin-22 mediates early host defense against attaching and effacing bacterial pathogens. Nat Med. 2008; 14:282–289. [PubMed: 18264109]
18. Eyerich S, et al. Th22 cells represent a distinct human T cell subset involved in epidermal immunity and remodeling. J Clin Invest. 2009; 119:3573–3585. [PubMed: 19920355]
19. Crellin NK, Trifari S, Kaplan CD, Cupedo T, Spits H. Human NKp44+IL-22+ cells and LTi-like cells constitute a stable RORC+ lineage distinct from conventional natural killer cells. J Exp Med. 2010; 207:281–290. [PubMed: 20142432]
20. Simonian PL, et al. gammadelta T cells protect against lung fibrosis via IL-22. J Exp Med. 2010; 207:2239–2253. [PubMed: 20855496]
21. Satoh-Takayama N, et al. Microbial flora drives interleukin 22 production in intestinal NKp46+ cells that provide innate mucosal immune defense. Immunity. 2008; 29:958–970. [PubMed: 19084435]
22. Satoh-Takayama N, et al. The natural cytotoxicity receptor NKp46 is dispensable for IL-22-mediated innate intestinal immune defense against Citrobacter rodentium. J Immunol. 2009; 183:6579–6587. [PubMed: 19846871]
23. Cella M, et al. A human natural killer cell subset provides an innate source of IL-22 for mucosal immunity. Nature. 2009; 457:722–725. [PubMed: 18978771]
24. Sanos SL, et al. RORgammat and commensal microflora are required for the differentiation of mucosal interleukin 22-producing NKp46+ cells. Nat Immunol. 2009; 10:83–91. [PubMed: 19029903]
25. Satoh-Takayama N, et al. IL-7 and IL-15 independently program the differentiation of intestinal CD3-NKp46+ cell subsets from Id2-dependent precursors. J Exp Med. 2010; 207:273–280. [PubMed: 20142427]
26. Colonna M. Interleukin-22-producing natural killer cells and lymphoid tissue inducer-like cells in mucosal immunity. Immunity. 2009; 31:15–23. [PubMed: 19604490]
27. Couceiro JN, Paulson JC, Baum LG. Influenza virus strains selectively recognize sialyloligosaccharides on human respiratory epithelium; the role of the host cell in selection of hemagglutinin receptor specificity. Virus Res. 1993; 29:155–165. [PubMed: 8212857]
28. Seo SU, et al. Type I interferon signaling regulates Ly6C(hi) monocytes and neutrophils during acute viral pneumonia in mice. PLoS Pathog. 2011; 7:e1001304. [PubMed: 21383977]
29. Kumar P, et al. High-throughput Detection Method for Influenza Virus. JoVE. 2012
30. Dhiman R, et al. IL-22 produced by human NK cells inhibits growth of Mycobacterium tuberculosis by enhancing phagolysosomal fusion. J Immunol. 2009; 183:6639–6645. [PubMed: 19864591]
31. Satoh-Takayama N, et al. Lymphotoxin-beta receptor-independent development of intestinal IL-22-producing NKp46+ innate lymphoid cells. Eur J Immunol. 2011; 41:780–786. [PubMed: 21341264]
32. Scriba TJ, et al. Distinct, specific IL-17- and IL-22-producing CD4+ T cell subsets contribute to the human anti-mycobacterial immune response. J Immunol. 2008; 180:1962–1970. [PubMed: 18209095]
33. Ma SD, Lancto CA, Enomoto S, Abrahamsen MS, Rutherford MS. Expression and regulation of IL-22 by bovine peripheral blood gamma/delta T cells. Gene. 2010; 451:6–14. [PubMed: 19879340]
34. Yao S, et al. Differentiation, distribution and gammadelta T cell-driven regulation of IL-22-producing T cells in tuberculosis. PLoS Pathog. 2010; 6:e1000789. [PubMed: 20195465]
35. Ness-Schwickerath KJ, Morita CT. Regulation and function of IL-17A- and IL-22-producing gammadelta T cells. Cell Mol Life Sci. 2011; 68:2371–2390. [PubMed: 21573786]
36. Huntington ND, et al. IL-15 trans-presentation promotes human NK cell development and differentiation in vivo. J Exp Med. 2009; 206:25–34. [PubMed: 19103877]
37. Liu CC, Perussia B, Young JD. The emerging role of IL-15 in NK-cell development. Immunol Today. 2000; 21:113–116. [PubMed: 10689297]
38. Mount AM, Belz GT. Mouse models of viral infection: influenza infection in the lung. Methods Mol Biol. 2010; 595:299–318. [PubMed: 19941121]

39. Buchweitz JP, Harkema JR, Kaminski NE. Time-dependent airway epithelial and inflammatory cell responses induced by influenza virus A/PR/8/34 in C57BL/6 mice. Toxicol Pathol. 2007; 35:424–435. [PubMed: 17487773]
40. Sentman CL, et al. Pan natural killer cell monoclonal antibodies and their relationship to the NK1.1 antigen. Hybridoma. 1989; 8:605–614. [PubMed: 2613267]
41. Luci C, et al. Influence of the transcription factor RORgammat on the development of NKp46+ cell populations in gut and skin. Nat Immunol. 2009; 10:75–82. [PubMed: 19029904]
42. Koka R, et al. Interleukin (IL)-15R[alpha]-deficient natural killer cells survive in normal but not IL-15R[alpha]-deficient mice. J Exp Med. 2003; 197:977–984. [PubMed: 12695489]
43. Nakamura R, et al. Interleukin-15 is critical in the pathogenesis of influenza a virus-induced acute lung injury. J Virol. 2010; 84:5574–5582. [PubMed: 20335267]
44. Chow KP, et al. Enhanced IL-10 production by CD4+ T cells primed in IL-15Ralpha-deficient mice. Eur J Immunol. 2011; 41:3146–3156. [PubMed: 21874651]
45. Yokoyama S, Takada K, Hirasawa M, Perera LP, Hiroi T. Transgenic Mice that Overexpress Human IL-15 in Enterocytes Recapitulate Both B and T Cell-Mediated Pathologic Manifestations of Celiac Disease. J Clin Immunol. 2011; 31:1038–1044. [PubMed: 21938511]
46. Kauffman SL. Cell proliferation in the mammalian lung. Int Rev Exp Pathol. 1980; 22:131–191. [PubMed: 7005143]
47. Rock JR, et al. Basal cells as stem cells of the mouse trachea and human airway epithelium. Proc Natl Acad Sci U S A. 2009; 106:12771–12775. [PubMed: 19625615]
48. Wolk K, Kunz S, Asadullah K, Sabat R. Cutting edge: immune cells as sources and targets of the IL-10 family members? J Immunol. 2002; 168:5397–5402. [PubMed: 12023331]
49. Zenewicz LA, et al. Innate and adaptive interleukin-22 protects mice from inflammatory bowel disease. Immunity. 2008; 29:947–957. [PubMed: 19100701]
50. Weiss LM, et al. Proliferative rates of non-Hodgkin's lymphomas as assessed by Ki-67 antibody. Hum Pathol. 1987; 18:1155–1159. [PubMed: 3679189]
51. Nakagome K, et al. High Expression of IL-22 Suppresses Antigen-Induced Immune Responses and Eosinophilic Airway Inflammation via an IL-10-Associated Mechanism. J Immunol. 2011; 187:5077–5089. [PubMed: 21998459]
52. Guo H, Topham DJ. Interleukin-22 (IL-22) production by pulmonary Natural Killer cells and the potential role of IL-22 during primary influenza virus infection. J Virol. 2010; 84:7750–7759. [PubMed: 20504940]
53. Wolk K, et al. IL-22 regulates the expression of genes responsible for antimicrobial defense, cellular differentiation, and mobility in keratinocytes: a potential role in psoriasis. Eur J Immunol. 2006; 36:1309–1323. [PubMed: 16619290]
54. Fernandez-Sesma A, et al. Influenza virus evades innate and adaptive immunity via the NS1 protein. J Virol. 2006; 80:6295–6304. [PubMed: 16775317]
55. Sanos SL, Diefenbach A. Isolation of NK cells and NK-like cells from the intestinal lamina propria. Methods Mol Biol. 2010; 612:505–517. [PubMed: 20033661]
56. Guo H, Samarakoon A, Vanhaesebroeck B, Malarkannan S. The p110 delta of PI3K plays a critical role in NK cell terminal maturation and cytokine/chemokine generation. J Exp Med. 2008; 205:2419–2435. [PubMed: 18809712]
57. Rajasekaran K, et al. Transforming Growth Factor-{beta}-activated Kinase 1 Regulates Natural Killer Cell-mediated Cytotoxicity and Cytokine Production. J Biol Chem. 2011; 286:31213–31224. [PubMed: 21771792]
58. Awasthi A, et al. Rap1b facilitates NK cell functions via IQGAP1-mediated signalosomes. J Exp Med. 2010; 207:1923–1938. [PubMed: 20733035]

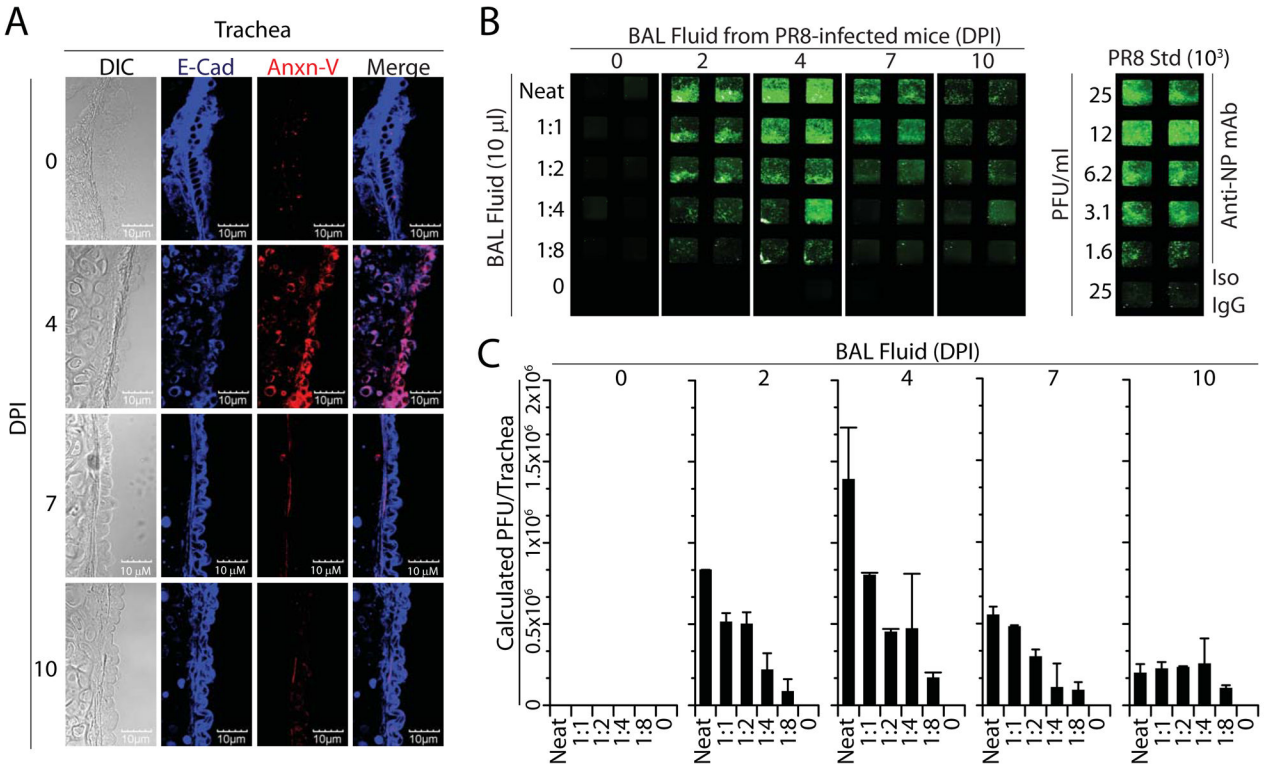

Figure 1. Tracheal epithelial cell death correlates with influenza viral titer

(**A**) Tracheal sections from PR8-infected mice were stained with anti-E-Cadherin (E-Cad, epithelial cells, blue), Annexin-V (Anxn-V, apoptotic cells, red) and are shown with Differential Interference Contrast (DIC) images. Data shown are one set of representative panels from a group of five mice infected with PR8 for each DPI and from a total of three different experiments. (**B**) Levels of PR8 viral titers were quantified using a novel infrared dye-based assay[29]. MDCK cells were incubated with BAL fluids from PR8-infected mice for 16 h. Nucleoprotein (NP) of influenza virus was detected in the infected MDCK cells using monoclonal anti-NP antibody. BAL fluids from five infected mice for each DPI were collected and analyzed, and data from one representative of five independent experiments are shown. (**C**) Influenza viral titers were quantified through a IR-dye based method using a standard curve. Data shown are averages of PFU from duplicate wells and a representative of five independent experiments.

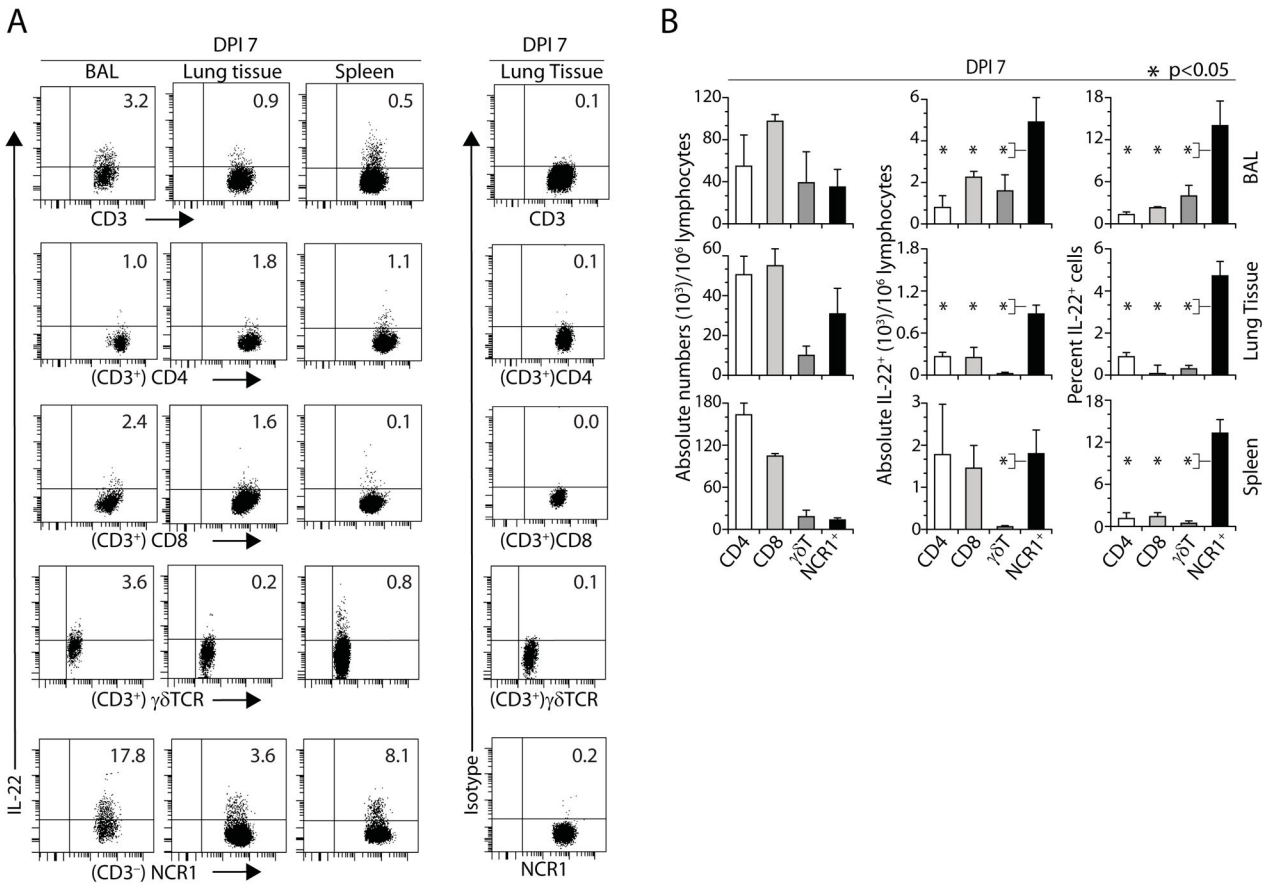

Figure 2. NCR1$^+$ cells predominantly generate IL-22 in the lung during influenza infections

(A) Single cell suspensions from indicated organs of infected mice were stained with anti-CD3, anti-CD4, anti-CD8, anti-γδTCR, anti-NCR1, and anti-IL-22 antibodies and analyzed through flow cytometry to define the cell populations that are positive for intracellular IL-22. Dot plots of IL-22$^+$ cells among CD3$^+$CD4$^+$ T, CD3$^+$CD8$^+$ T, CD3$^+$γδTCR$^+$ T and CD3$^-$NCR1$^+$ cells are shown. Data shown in (A) are one representative of six mice analyzed on DPI 7. (**B**) Absolute numbers and percentages of total and IL-22$^+$ cell types based on CD3$^+$CD4$^+$, CD3$^+$CD8$^+$, CD3$^+$γδTCR$^+$ T, or NCR1$^+$ gating in various organs on DPI 7. Data shown in (B) are averages and standard deviations of six mice each and one of three independent experiments. Asterisks in (B) denote: *=p<0.05.

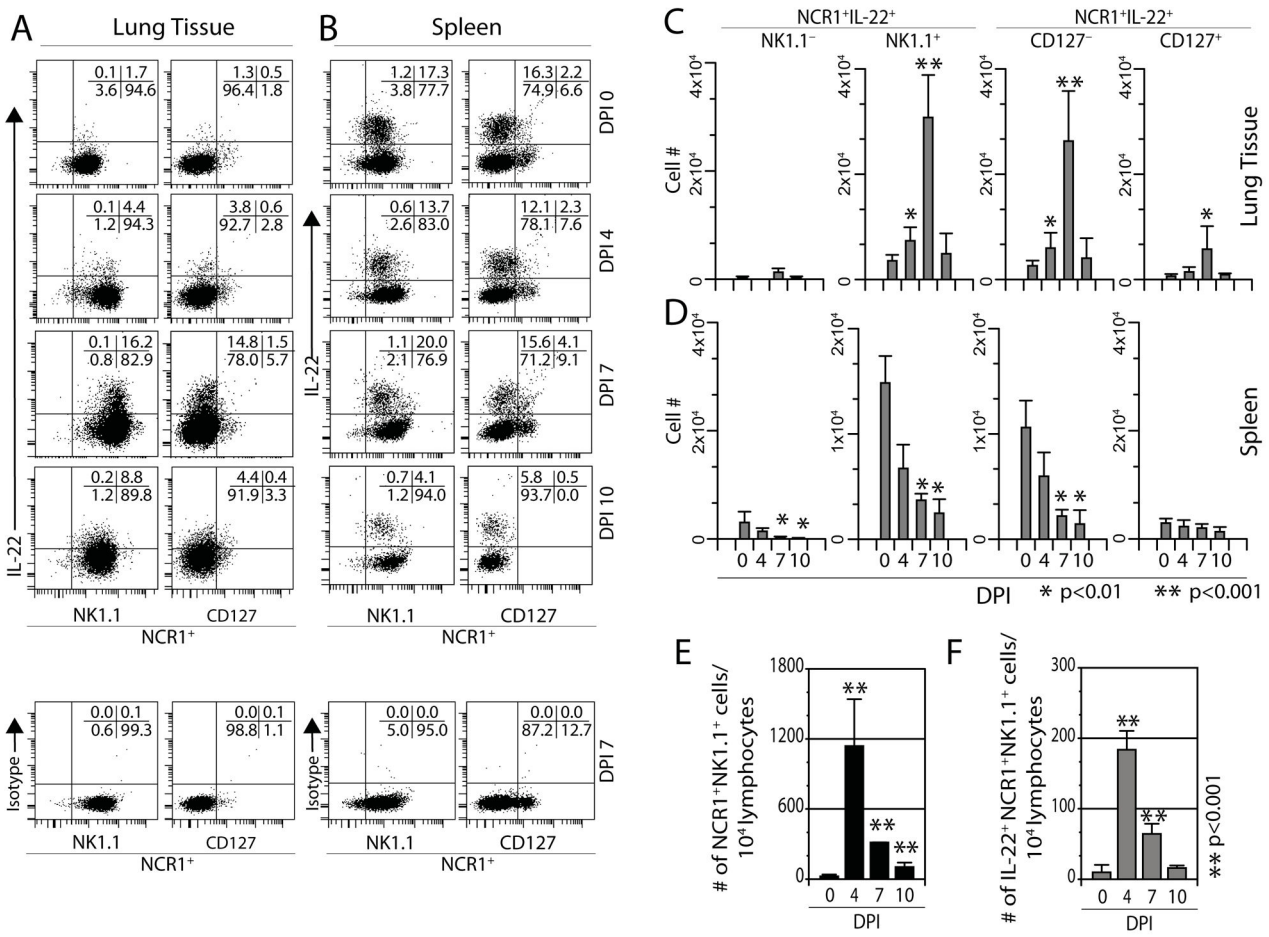

Figure 3. IL-22-producing NCR1$^+$ cells in the influenza-infected lungs are conventional NK cells

Phenotypes of IL-22-generating NCR1$^+$ cells and their absolute numbers are shown. Flow cytometry analyses of IL-22$^+$ cells from (**A**) lung tissue or (**B**) spleen from mice at different DPI are shown. Single cell suspensions were stained for CD3, NCR1, NK1.1, CD127 and intracellular IL-22. CD3$^-$NCR1$^+$ cells were gated and analyzed for IL-22/Isotype and NK1.1 or IL-22/Isotype and CD127. Individual dot plots (**A,B**) or average absolute numbers (**C,D**) of IL-22 producing NCR1$^+$ cells are shown. Data shown are one representative (A,B) and average absolute numbers with standard deviations (C,D,) of five mice for each DPI. Data shown in A and B are from one representative of three independent experiments. (**E**) Absolute numbers of total and **(F)** IL-22$^+$NCR1$^+$NK1.1$^+$ cells on indicated DPI in the trachea of infected mice. Cell numbers were calculated and shown per 10,000 total lymphocytes. Data shown in E, F are the averages with standard deviations of six mice each from three independent experiments. Asterisks in (C–F) denote: *=p<0.01 and **= p<0.001.

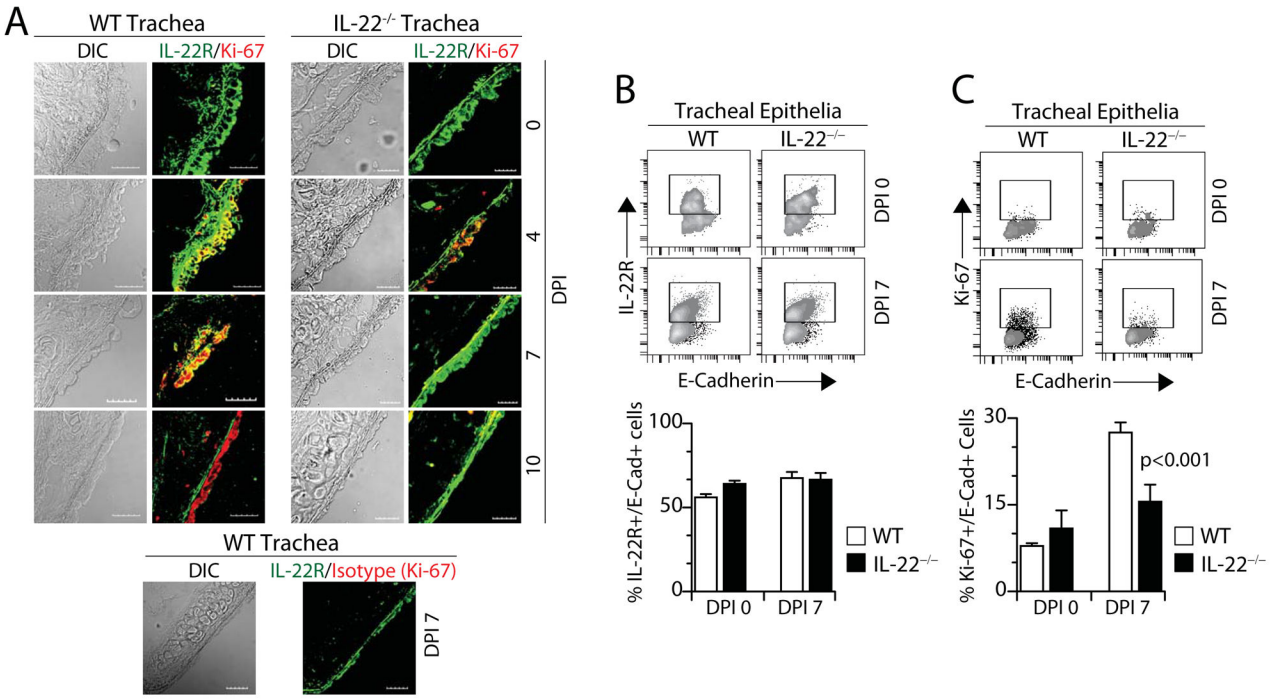

Figure 4. Lack of IL-22 significantly reduces the proliferation of tracheal epithelial cells

(**A**) Tracheal sections from infected mice on different DPI were stained with anti-IL-22R, anti-Ki-67 or isotype antibodies and analyzed using confocal microscopy. Data shown are one representative of a minimum of three independent experiments with three mice each DPI. (**B**) Flow cytometric analyses of IL-22R expression by tracheal epithelial cells or of (**C**) Ki-67 in influenza-infected WT and *IL-22*$^{-/-}$ mice on DPI 0 and 7. Data presented averages and standard deviations of percent IL-22R or Ki-67 positive epithelial cells (E-Cadherin^{+}) were calculated from three of WT and *IL-22*$^{-/-}$ mice each.

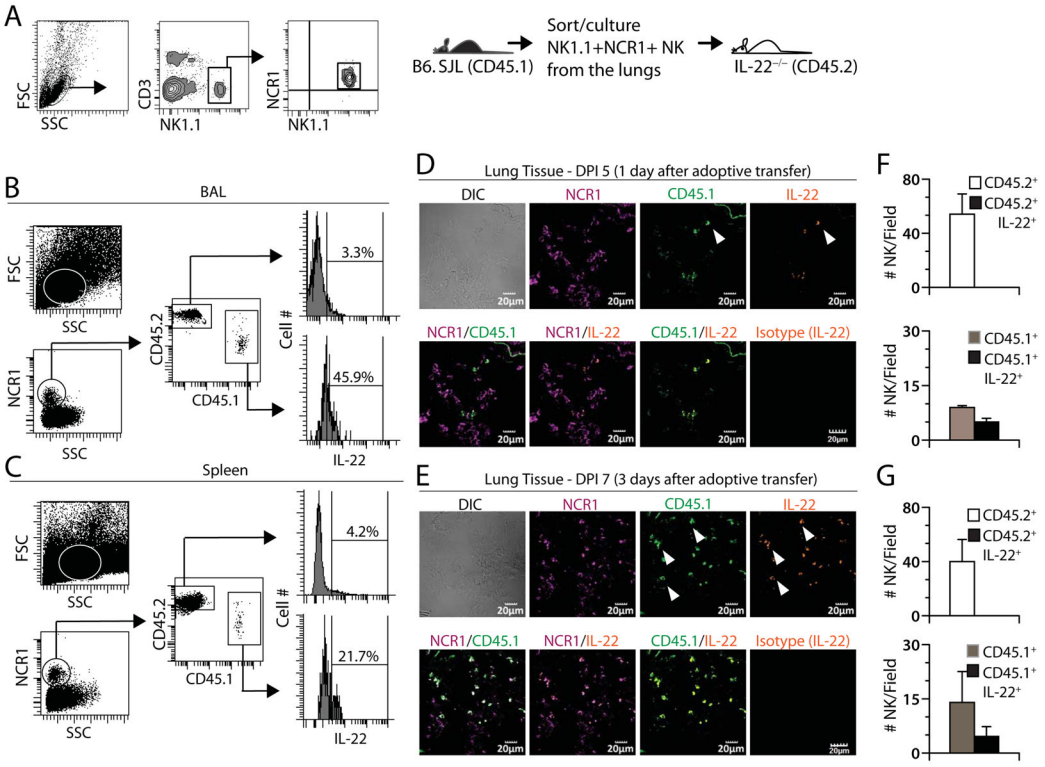

Figure 5. Adoptive transfer and detection of IL-22-producing NK cells in *IL-22*$^{-/-}$ mice

(A) Sorting schema for CD3^{-}NK1.1^{+}NCR1^{+} NK cells. CD45.1^{+} lung-derived lymphocytes from B6.SJL mice (H-2^{b}) were stained with anti-CD3, anti-NK1.1 and anti-NCR1 antibodies and the CD3^{-}NK1.1^{+}NCR1^{+} NK cells were sorted and cultured with IL-2 for 8–12 days before they were adoptively transferred intravenously into *IL-22*$^{-/-}$ mice (H-2^{b}, CD45.2^{+}) on DPI 4 of influenza infection. (**B**) BAL fluid and (**C**) spleens of the host *IL-22*$^{-/-}$ mice were tested for donor-derived IL-22-generating NK cells. Lungs from the host mice were analyzed through confocal microcopy for the presence of CD45.1^{+} IL-22-producing NK cells after (**D**) one or (**E**) three days of adoptive transfer. (**F,G**) Quantification of IL-22-producing NK cells in (D) and (E). IL-22^{+}CD45.1^{+} or IL-22^{+}CD45.2^{+} NK cells were counted in 10 independent fields per combination and are shown as averages with standard deviations.

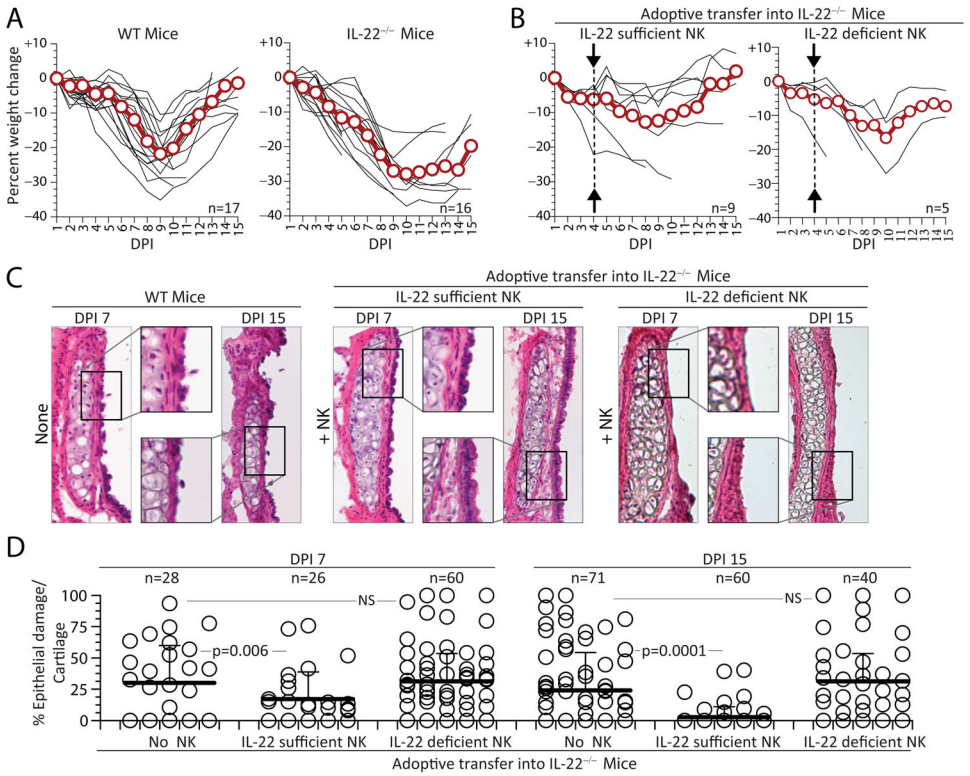

Figure 6. Adoptively transferred IL-22 sufficient but not IL-22 deficient NK cells promote epithelial cell regeneration in *IL-22*$^{-/-}$ mice

(A,B) Weight loss after influenza infection was monitored in WT and in *IL-22*$^{-/-}$ mice with or without the adoptive transfer of NK cells. Weight loss in individual mice is represented by lines and the average values are shown in red circles. Data presented were from a total of 17 WT and 16 *IL-22*$^{-/-}$ with no adoptive transfer and 5–9 mice with adoptive transfer. Arrows indicate the time of adoptive transfer of NK cells into *IL-22*$^{-/-}$ mice. (**C, D**) Integrity of tracheal epithelial cell layers after adoptive transfer of IL-22-sufficient or deficient NK cells into *IL-22*$^{-/-}$ mice. (**C**) Hematoxylin and Eosin staining of trachea from WT and *IL-22*$^{-/-}$ mice on indicated DPI that were adoptively transferred with IL-22 sufficient or IL-22 deficient NK cells. Exploded views are shown for details. (**D**) Epithelial cell damage per cartilage length was calculated from 3–6 mice for each DPI and presented with p values and NS denotes not significant. ‘n’ denotes the number of cartilages analyzed for each group.

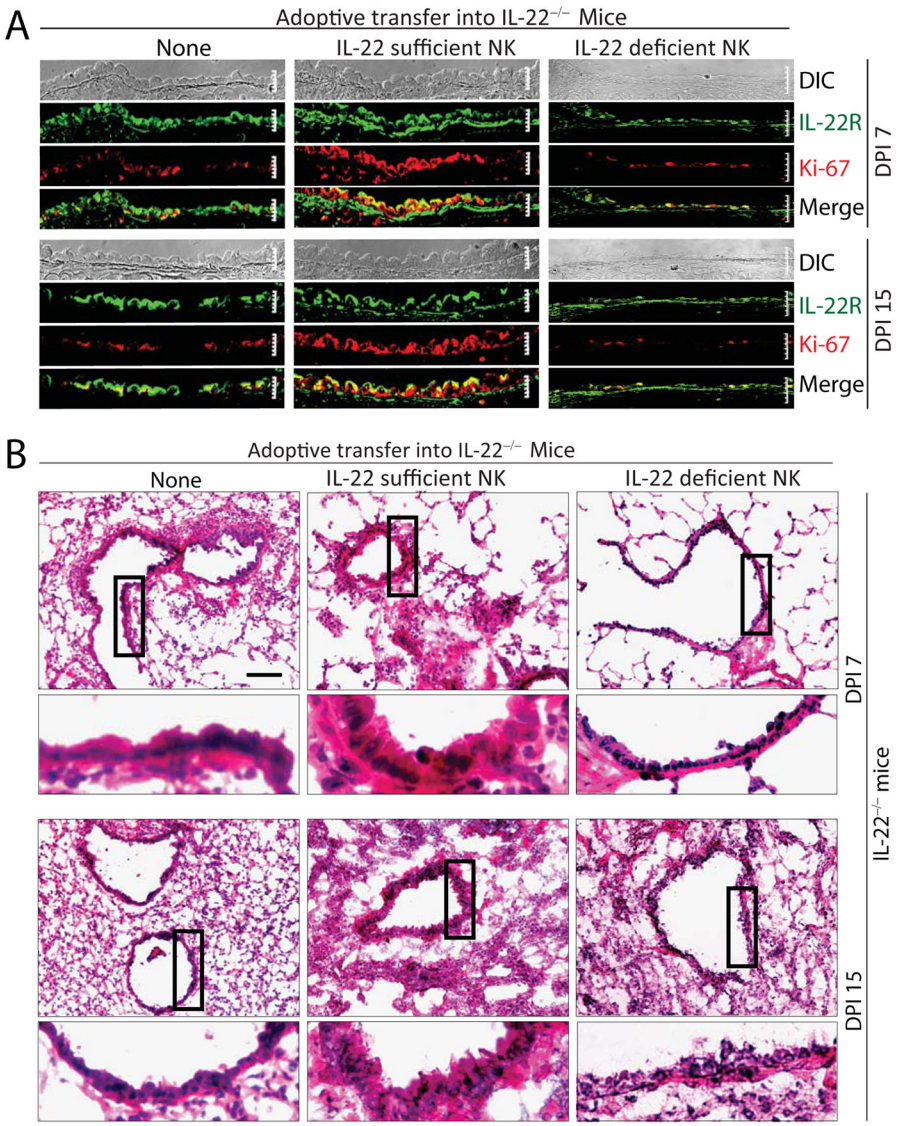

Figure 7. Adoptive transfer of IL-22 sufficient NK cells augments epithelial cell proliferation in *IL-22*$^{-/-}$ mice

(**A**) Tracheal sections from *IL-22*$^{-/-}$ mice with or without the adoptive transfer of NK cells were immunostained with anti-IL-22R and anti-Ki-67. Data shown are representatives of confocal images from indicated mice. Tracheae were collected after indicated DPI. White scale bars in each confocal image represent five microns. (**B**) Lungs from the *IL-22*$^{-/-}$ mice with or without adoptive transfer of IL-22 sufficient or IL-22 deficient NK cells were sectioned and stained with Hematoxylin and Eosin to analyze the regeneration of bronchial epithelial cells on indicated DPI. Photomicrographs of selected areas of apical lobes of the lungs show the levels of epithelial cell regeneration in the lumen side of the bronchia. Boxes denote the area selected and magnified. The black bar in the top left panel represents a scale of 100 micron. Data presented were from a total of at least three mice for each DPI from one of three independent experiments.

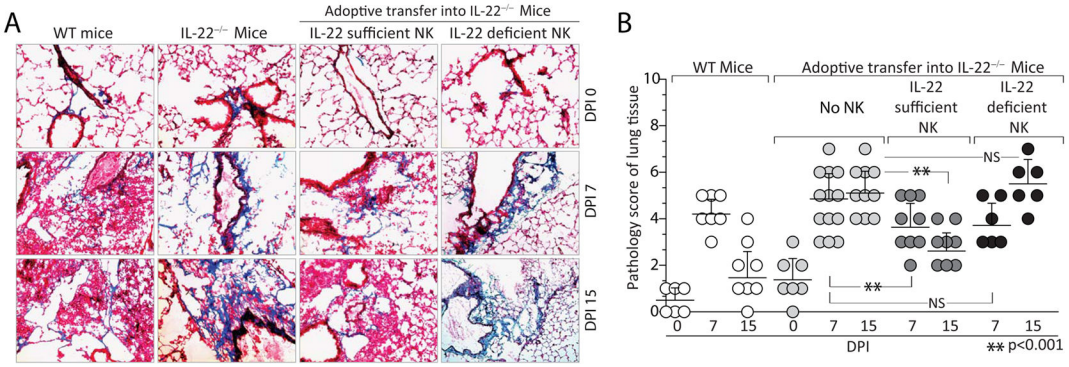

Figure 8. Lack of IL-22 increases lung inflammation

(**A**) Severity of inflammation after adoptive transfer of IL-22-sufficient or IL-22 deficient NK cells as visualized by collagen deposition (Mason's trichrome staining, blue) in the lung tissue. (**B**) Quantification of the degree of inflammation in the lung tissues on indicated DPI. Levels of collagen deposition were determined by a double-blind assay with a scale of 1–10, with 10 being severe. Data shown were collected from a total of 3–6 mice per DPI and were representatives of a minimum of three independent experiments. Asterisks in (B) denote: **=p<0.001 and NS= not significant.